

# Solvatochromic shifts of single-walled carbon nanotubes in nonpolar microenvironments†

Carlos A. Silvera-Batista,<sup>a</sup> Randy K. Wang,<sup>a</sup> Philip Weinberg<sup>a</sup> and Kirk J. Ziegler<sup>\*abc</sup>

Received 22nd December 2009, Accepted 5th March 2010

First published as an Advance Article on the web 12th May 2010

DOI: 10.1039/b927053a

Single-walled carbon nanotubes (SWNTs) are encapsulated with microenvironments of nonpolar solvent, providing a new method to measure the photophysical properties of nanotubes in environments with known properties. Photoluminescence (PL) and absorbance spectra of SWNTs show solvatochromic shifts in 16 nonpolar solvents, which are proportional to the solvent induction polarization. The shifts in the emission energies ( $\Delta E_{11}$ ) range from approximately 25 to 100 meV and the smallest diameter SWNTs have the largest shifts. The PL intensity of SWNTs is very sensitive to changes in polarity. For example, SWNTs encapsulated with chloroform ( $\epsilon \sim 5$ ) show substantial reductions in intensity. The solvatochromic shifts of SWNTs were used to determine the relationship between the longitudinal polarizability, band gap and radius,  $\alpha_{L,\parallel} \propto 1/(R^2 E_{11}^3)$ .

## Introduction

Single-walled carbon nanotubes (SWNTs) have characteristic optical transition energies ( $E_{ii}$ ) associated with their ( $n,m$ ) chirality. The  $E_{ii}$  associated with each SWNT ( $n,m$ ) type were assigned by dispersing nanotubes with the aid of surfactants,<sup>1–3</sup> enabling characterization through absorbance and photoluminescence (PL) spectroscopy.<sup>4,5</sup> Typically, sodium dodecyl sulfate (SDS), sodium dodecylbenzene sulfonate (SDBS), and sodium cholate (SC) are used to suspend SWNTs, although other surfactants are also used.<sup>1–3,6</sup>

While these studies have facilitated the application and understanding of SWNTs, the effect of the environment surrounding the nanotubes on SWNT properties is still not well understood.<sup>7–17</sup> The inability to suspend SWNTs in known dielectric environments, such as organic solvents, complicates these studies.<sup>18</sup> Several studies have used nanotubes suspended across trenches to study environmental effects on SWNT PL emission;<sup>13–15</sup> however, mechanical strain and charge transfer can effect the measurements.<sup>15,19</sup> The limited understanding of environmental effects on SWNT properties is also partially due to the unknown or poorly characterized surfactant structure,<sup>20,21</sup> which makes it difficult to assess the dielectric constant of the media surrounding SWNTs.

The polarizability of individual SWNTs is also important to many applications as well as the photophysical and photochemical response of SWNTs. The polarizability is highly anisotropic with the longitudinal component ( $\alpha_{\parallel}$ ) at least an order of magnitude larger than the transverse component ( $\alpha_{\perp}$ ). Therefore, the longitudinal polarizability is the dominant

contribution and the dipole moment is oriented along the nanotube axis. Several models have been developed to calculate the longitudinal polarizability. These models suggest the longitudinal polarizability is a function of the nanotube radius ( $R$ ) and band gap energy of SWNTs but disagree on the relationship. Researchers have found theoretical relationships where the longitudinal polarizability is proportional to either  $R/(E_{ii})^2$ ,  $1/E_{ii}$ ,  $1/(E_{ii})^2$ , or  $R^2$ .<sup>22–25</sup>

While there are several theoretical studies on the polarizability of SWNTs, there are few experimental studies.<sup>9,26</sup> Measuring the photophysical properties of molecules, such as solvatochromic shifts, can provide information about the excited states of the molecules and even their polarizability. Choi and Strano used solvatochromic shifts of SWNTs to determine that longitudinal polarizability varies with  $1/R(E_{ii})^2$ .<sup>9</sup> However, these measurements were based on relatively few systems, including surfactant-suspended SWNTs, whose dielectric environments are still not well characterized.

The theoretical and experimental studies described above show that the exact form of the longitudinal polarizability remains unknown. Experimental measurement of solvatochromic shifts in a variety of solvents remains a good approach to study polarizability, provided that SWNTs can be suspended in several solvents of known dielectric constant. However, dispersing SWNTs in organic solvents remains a challenging task.<sup>18</sup> Recently, our group has observed that mixing a suspension containing SDBS-coated SWNTs with immiscible organic solvents induces solvatochromic shifts or dielectric screening effects, which are dependent on the solvent.<sup>27</sup> The PL spectra of SDBS-SWNT suspensions mixed with *o*-dichlorobenzene (ODCB) showed identical shifts to the PL from SWNTs suspended in only ODCB (*i.e.* no surfactant or water).<sup>18</sup> The similarity in the peak positions indicates that the hydrophobic core of the surfactant forms an emulsion-like microenvironment of ODCB around the nanotube. Here, we use these new microenvironments around SWNTs to investigate the photophysical properties of SWNTs in a variety of solvents. While the presence of the organic solvent can modify

<sup>a</sup> Department of Chemical Engineering, University of Florida, Gainesville, Florida 32611

<sup>b</sup> Department of Materials Science and Engineering, University of Florida, Gainesville, Florida 32611

<sup>c</sup> Center for Surface Science and Engineering, University of Florida, Gainesville, Florida 32611. E-mail: kziegler@che.ufl.edu

† Electronic supplementary information (ESI) available: Deconvolution of the spectra; solvent characterization sheets. See DOI: 10.1039/b927053a

the surfactant assembly around the SWNT surface<sup>27</sup> and subsequently affect the PL emission,<sup>28–30</sup> the present work uses SDBS as the surfactant, which has minimal rearrangement of the surfactant structure in the presence of organic solvents.<sup>27</sup> The solvatochromic shifts follow the expected behavior from a polarizable solute in a polarizable solvent. The PL intensity is shown to be very sensitive to polar solvents. Relationships are developed to describe the solvatochromic shifts and PL intensity of different (*n,m*) types in low dielectric media.

## Experimental

### Reagents

Deionized water was used in all experiments. The surfactant, sodium dodecylbenzene sulfonate (SDBS), was obtained from Sigma-Aldrich (St. Louis, MO, USA) and used as received (Technical Grade). HiPco SWNTs were obtained from Rice University (Rice HPR 145.1) and used as received. The nonpolar solvents examined in this study were obtained from Sigma-Aldrich (hexane (99%), heptane (99%), cyclohexane (99%), carbon tetrachloride (99.9%), 1-chlorohexane (99%), 1,6-dichlorohexane (98%), 2-heptanol (98%), 3-heptanol (99%), 1-chlorobutane (99.8%), 2,6-dichlorotoluene (99%), 3,4-dichlorotoluene (97%), o-dichlorobenzene (99%)), Fisher Scientific (Pittsburgh, PA, USA) (chloroform (99.8%), p-xylene (99.7%), toluene (99%)) and Fluka (benzene (99.5%), 1,3-dichlorobenzene (99%)). All solvents were used as received.

### Aqueous SWNT suspensions

All experiments used SDBS since this surfactant did not show any quenching effects upon mixing with organic solvents, as observed for SDS-SWNT suspensions.<sup>27</sup> Aqueous suspensions of nanotubes were prepared by mixing 20 mg of raw SWNTs with 200 mL of a SDBS solution (1 wt%). High-shear homogenization (IKA T-25 Ultra-Turrax) for 1.5–2 h and ultrasonication (Misonix S3000) for 10 min were used to aid dispersion. After ultrasonication, the mixture was ultracentrifuged at 20000 rpm for 5 h (Beckman Coulter Optima L-80 K).

## Solvent microenvironments around SWNTs

Immiscible solvents were added to each SWNT suspension (solvent : water volume ratio of 0.5) and mixed. The dielectric constant, refractive index, dipole moment, and induction polarization for each solvent is given in Table 1. The mixture was shaken vigorously for 30 s with a vortex stirrer. A white emulsion phase immediately started to coalesce after shaking. After waiting for 1.5–2 h to reach steady state, the excess organic solvent was then carefully removed from the aqueous SWNT suspension without promoting further emulsification.

### SWNT characterization

The aqueous phase was characterized by vis-NIR absorbance and NIR-fluorescence spectroscopy using an Applied NanoFluorescence Nanospectralyzer (Houston, TX) with excitation from 662 and 784 nm diode lasers. Although the organic solvents have some absorbance bands in the NIR region (see electronic supplementary information†), their effect on the spectral properties were determined to be minor. This conclusion is supported by the fact that no changes to the absorbance spectra of SWNTs are observed, which is consistent with a very small volume of solvent in the system. Likewise, absorption of SWNT photoluminescence (PL) by the solvent was concluded to have minimal effects on the PL emission intensity. All solvatochromic shifts are described relative to their emission energy in air, *i.e.*  $\Delta E_{11} = E_{11}^{\text{solvent}} - E_{11}^{\text{air}}$ .

### Deconvolution of PL spectra

SWNT PL spectra contains information on the  $E_{11}$  interband transitions for each (*n,m*) SWNT type. All PL spectra were deconvoluted into their respective bands for each (*n,m*) type using the Applied Nanospectralyzer software (Houston, TX). The deconvolution routine uses Voigt profiles for each (*n,m*) peak. Changes to the position ( $E_{11}$ ) and width of each (*n,m*) peak were limited to 0.1% and 3%, respectively, for each iteration to prevent the misidentification of peaks. After several iterations, the mean standard deviation (MSD) between the simulated and experimental data points was smaller than 0.005 (MSD < 0.005). Fig. S1† shows a typical spectra, which is deconvoluted into the peaks corresponding to each (*n,m*)

**Table 1** Properties of solvents used to form microenvironments around SWNTs

Solvents	Relative dielectric constant <sup>a</sup>	Refractive index <sup>a</sup>	Dipole moment/D	Induction polarization $f(\eta^2)$
Hexane	1.89	1.37	0.00 <sup>a</sup>	0.369
Heptane	1.92	1.39	0.00 <sup>a</sup>	0.383
Cyclohexane	2.02	1.43	0.00 <sup>a</sup>	0.411
Carbon tetrachloride	2.23	1.46	0.00 <sup>a</sup>	0.430
p-Xylene	2.27	1.50	0.00 <sup>a</sup>	0.455
Benzene	2.28	1.50	0.00 <sup>a</sup>	0.455
Toluene	2.39	1.50	0.38 <sup>a</sup>	0.455
2,6-Dichlorotoluene	3.36	1.55	0.83 <sup>b</sup>	0.483
Chloroform	4.81	1.45	1.04 <sup>a</sup>	0.424
1-Chlorohexane	6.10	1.42	1.94 <sup>a</sup>	0.404
3-Heptanol	7.07	1.42	1.71 <sup>a</sup>	0.404
1-Chlorobutane	7.28	1.40	2.05 <sup>a</sup>	0.390
1,6-Dichlorohexane	8.60	1.46	2.03 <sup>c</sup>	0.430
3,4-Dichlorotoluene	9.39	1.55	3.00 <sup>a</sup>	0.483
2-Heptanol	9.72	1.42	1.71 <sup>a</sup>	0.404
o-Dichlorobenzene	10.12	1.55	2.50 <sup>a</sup>	0.483

<sup>a</sup> Properties taken from CRC Handbook of Chemistry and Physics.<sup>39</sup> <sup>b</sup> Property taken from Calderbank *et al.*<sup>40</sup> <sup>c</sup> Property taken from Vaughan *et al.*<sup>41</sup>

type. The peak position of every  $(n,m)$  type of SWNTs after deconvolution is used in the nonlinear optimization model.

## Results and discussion

### Solvatochromic shifts of SWNT spectra in various solvents

Fig. 1a and b show the PL emission spectra of SWNTs excited with a 662 and 784 nm laser, respectively, when mixed with a variety of nonpolar solvents with different dielectric constants, refractive indices, and polarities (see Table 1). All features of the spectra show peak shifts as well as intensity changes with each solvent. SWNT suspensions mixed with hexane show the highest PL intensity and emission energy. In contrast, SWNT suspensions mixed with ODCB have lower PL intensity and red-shifted peak positions. Fig. 1c shows similar peak shifts in the absorbance spectra of SWNTs in the same solvents.

To see the spectral changes more clearly, Fig. 2a and b show the PL spectra corresponding to only the (7,6) and (10,5) SWNT types when mixed with the nonpolar solvents. The figures show changes in both the intensity and peak position as the solvent is altered from hexane to ODCB. These different environments show that, in general, the emission energy tends to red-shift and the intensity decreases as the dielectric constant (solvent polarity) is increased. However, there are some deviations in the trends. For example, 2,6-dichlorotoluene and 2-heptanol are red- and blue-shifted more than solvents with similar dielectric constants, respectively. In addition, the peak widths get broader in high polarity solvents, such as 3,4-dichlorotoluene and ODCB. The absorbance spectra for both the  $E_{11}$  and  $E_{22}$  transitions of the (7,6) SWNT are shown in Fig. 2c and d and also show similar spectral shifts as the solvent polarity is increased. However, the  $E_{11}$  (0.85–1.4 eV) transitions of the SWNTs are more sensitive to the solvent environments (larger shifts) than the  $E_{22}$  (1.4–2.1 eV) transitions, in agreement with prior observations.<sup>9</sup>

The peak shifts in the spectra of Fig. 1 and 2 indicate that SWNTs are experiencing different environments when mixed with nonpolar organic solvents. SWNTs have no net dipole moment but are highly polarizable. Prior to photo-excitation, the solvent induces a small reaction field on the SWNTs (dielectric screening) and *vice versa*. The field changes the

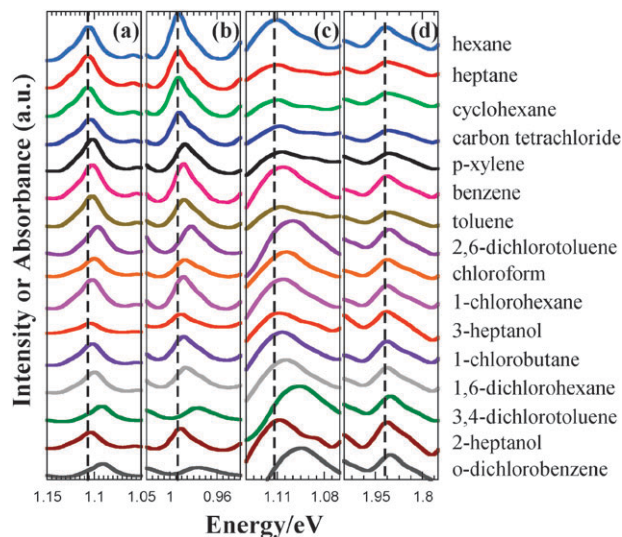


**Fig. 2** PL spectra ( $E_{11}$  emission) for the (a) (7,6) and (b) (10,5) SWNT species and (c)  $E_{11}$  and (d)  $E_{22}$  absorbance for the (7,6) SWNT type measured in microenvironments of various nonpolar solvents. The lines are the peak position for SWNTs in hexane microenvironments.

solvation energy associated with stabilizing the ground state, yielding characteristic absorption energies (solvatochromic shifts) in different solvents. The excited state of SWNTs should have a larger dipole moment after photon absorption, generating a field that forces the solvent structure to rearrange or relax around the excited state SWNT dipole. According to the Franck–Condon principle, solvent reorientation is too slow to be observed during absorption but can be observed in PL emission. Each solvent responds differently to the excited state dipole, resulting in solvatochromic shifts of the PL emission of SWNTs that may differ from those observed in absorbance. The observed spectral changes in Fig. 1 and 2 suggest the measured solvatochromic shifts are due to the formation of a solvent microenvironment encapsulating the SWNTs.<sup>27</sup>

Fig. 3a shows a schematic of the microenvironments formed around SWNTs based on these results as well as prior spectroscopic observations (summarized in Fig. 3b).<sup>27</sup> The initial surfactant structure has the SDBS molecules on the sidewall

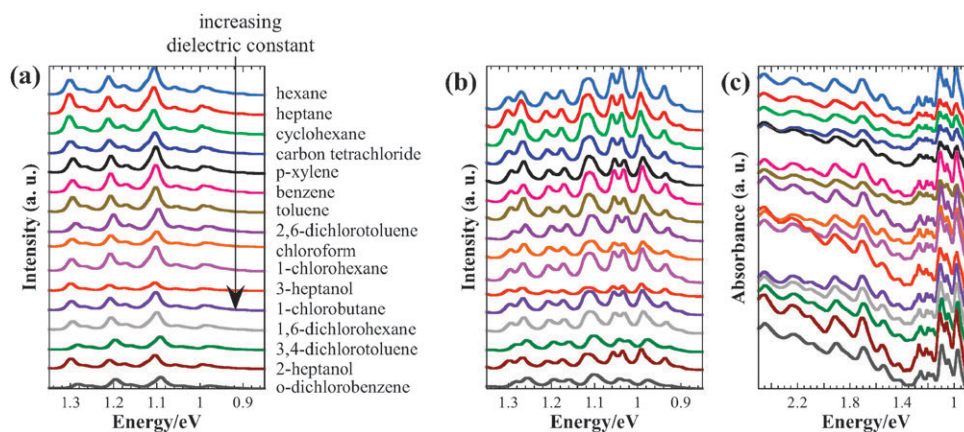


**Fig. 1** PL emission spectra of SWNTs excited at (a) 662 and (b) 784 nm and (c) absorbance spectra of SWNTs in nonpolar microenvironments. All spectra in a–c are offset for clarity and arranged by dielectric constant.

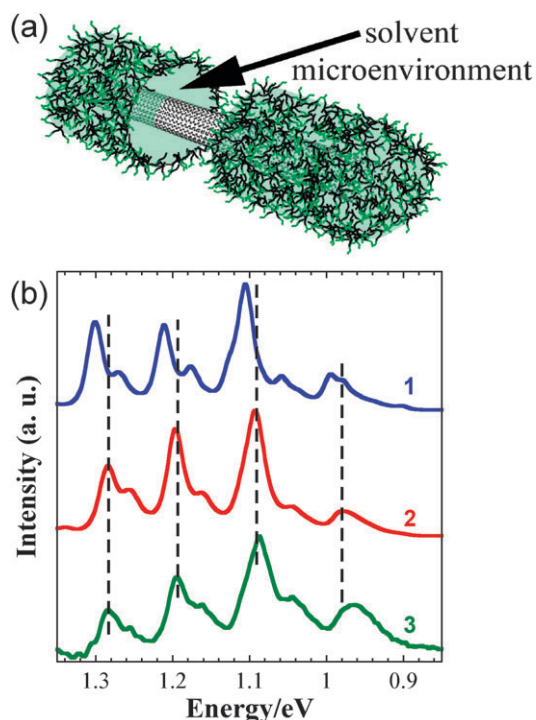


**Fig. 3** (a) Schematic of the nonpolar solvent microenvironments formed around SWNTs. The cut-out section shows the solvent layer encases the nanotube, providing an approach to systematically alter the environment surrounding SWNTs. (b) Comparison of PL emission spectra (ex. = 662 nm) of SWNTs surrounded by (1) SDBS surfactant, (2) ODCB microenvironments, and (3) pure ODCB. Dashed lines show the emission energy for select  $(n,m)$  species. Note that the positions for (2) and (3) are consistent confirming that the spectroscopic results for microenvironments around SWNTs are similar to dispersions in pure solvent. The similarity in peak positions also indicates that the surfactant has a minor effect.<sup>27</sup>

of the SWNTs. However, after mixing with nonpolar solvents, the hydrophobic region between the SWNT sidewall and the surfactant swells, creating a small microenvironment of solvent. It was shown previously that the surfactant structure could be different in the presence of some organic solvents; however, these changes occurred when SDS was used to suspend the SWNTs and are easily observed by significant quenching of the PL.<sup>27</sup> Solvents that yielded similar behavior in the SDBS-SWNTs studied here, such as *m*-dichlorobenzene and ethyl acetate, were excluded from further analysis. Further, our prior work showed that PL emission energies of SWNTs in an ODCB microenvironment were identical to SWNTs in ODCB alone (see Fig. 3b). Therefore, the thickness of the shell is assumed to be large enough that the effects from the surfactant and water can be neglected. The fact that the PL spectra return to their original peak positions and intensity after the solvent is removed (not shown) suggests that aggregation is minimal, as discussed previously.<sup>27</sup>

### Characterizing solvatochromic shifts of SWNTs in nonpolar microenvironments

Researchers have related the environmental effects or solvatochromic shifts ( $\Delta E_{11}$ ) of SWNTs to the dielectric constant of

the environment.<sup>11,13,14</sup> These shifts were found to be approximately linear with the dielectric constant in low dielectric media, such as the solvents used in this study.<sup>13</sup> Fig. 4a shows the measured PL peak shifts from the data in Fig. 1 relative to air for multiple  $(n,m)$  types as a function of dielectric constant. Although the (9,7) nanotube has a reasonable linear fit to the dielectric constant of the solvent, most other nanotubes, especially small diameter nanotubes, show considerable scatter, such as the (6,5) and (8,3). Indeed, Miyauchi *et al.*<sup>13</sup> found significant deviations from linearity for SWNT PL measured in hexane ( $\epsilon = 1.89$ ).

The solvents used for these experiments are all considered to be nonpolar because of the relatively low dielectric constants.<sup>31</sup> Therefore, the solvatochromic shifts for each solvent are primarily influenced by the polarizability–polarizability interactions given by:<sup>32,33</sup>

$$\Delta E_{11} = E_{11}^{\text{solvent}} - E_{11}^{\text{air}} = -C_{\text{solvent}} \frac{\Delta\alpha_{11}}{\beta\gamma a^3} \Delta f_{\text{solvent-air}} \quad (1)$$

where  $C_{\text{solvent}}$  is a fluctuation parameter associated with SWNT dispersion forces,  $\Delta\alpha_{11}$  is the change in polarizability of SWNTs between the ground and excited states,  $\beta$  is a shape factor for the SWNT,  $\gamma$  is a parameter associated with the location of the SWNT dipole in the volume  $a^3$ , and  $\Delta f$  is the solvent induction polarization described by the Onsager polarity functions,  $f(\eta^2) = 2(\eta^2 - 1)/(2\eta^2 + 1)$ , where  $\eta$  is the refractive index of the solvent.<sup>32,33</sup> Fig. 4b shows the shifts plotted as a function of  $f(\eta^2)$ . As expected from eqn (1), the solvatochromic shifts in Fig. 4b tend to be linear for all  $(n,m)$  types, yielding significantly better  $R^2$  values than the relationship with dielectric constant.

The solvatochromic shifts range from approximately 20 meV for SWNTs with the largest diameters to as high as 100 meV for small diameter nanotubes. A direct comparison with the data from Ohno *et al.*<sup>14</sup> for the larger diameter (9,7), (10,5), (11,3), and (12,1) SWNT types in hexane and chloroform show excellent agreement to within a few meV. The similarity in spectral shifts strongly support the formation of a solvent microenvironment around the SWNTs, as shown in Fig. 3. As seen in Fig. 4c, the average solvatochromic shift for each  $(n,m)$  type in all solvents varies linearly with the inverse diameter ( $1/d$ ) of the nanotubes. No dependency of the spectral shift with the  $(n-m) \bmod 3$  value is observed. A least squares fit of the data in Fig. 4c yields an expression for the average shift as a function of nanotube diameter,  $\Delta E_{11}$  (eV) =  $0.076 - 0.119/d$  (nm). This simple expression excludes specific solvent effects but provides an estimate of the anticipated solvatochromic shift of SWNTs in low dielectric media.

While the peak positions are described better by the induction polarization of the solvent, the PL emission intensity is clearly a function of the dielectric constant of the solvent. As seen in Fig. 5a, the PL intensity decays rapidly as the dielectric constant increases. The trend is smooth and continuous until  $\epsilon \sim 5$ , where the data starts to scatter as the dielectric constant continues to increase. However, it is still clear that the intensity continues to decay as the dielectric is increased. Some of these intensity differences could be due to concentration differences between suspensions or removal of a small amount of aggregates at the interface.<sup>34,35</sup> Due to the large deviations

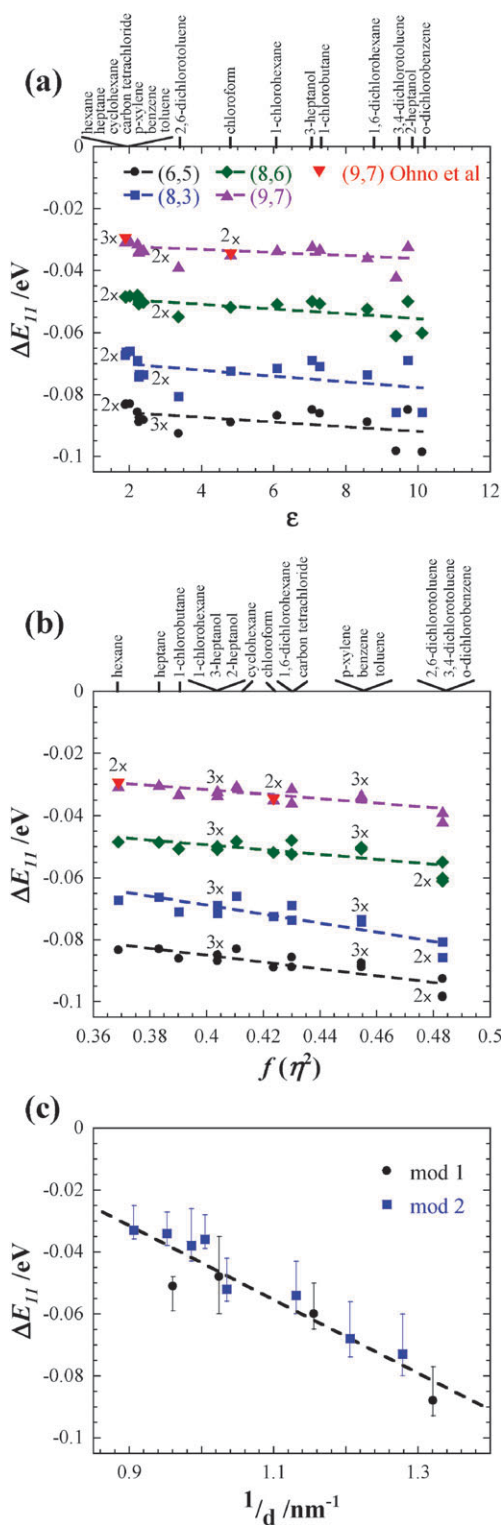


**Fig. 4** Solvatochromic shifts of various  $(n,m)$  SWNT types in non-polar solvents as a function of (a) dielectric constant and (b) solvent induction polarization,  $f(\eta^2)$ . Shifts observed for the (9,7) SWNT type by Ohno *et al.*<sup>14</sup> are also plotted for comparison. Note that there are multiple data points that are indistinguishable in (b). (c) Generalized solvatochromic shifts as a function of the inverse diameter of the SWNTs ( $1/d$ ). Note that the (11,1) and (9,4) SWNT types were excluded from (c) because of difficulties associated with deconvoluting them from the spectra.

associated with the intensity of 1-chlorohexane and 3-heptanol, these were excluded from power law fits to the intensity. The intensity of the SWNT PL emission was approximately proportional to  $\epsilon^{-0.5}$ .

The intensities of each  $(n,m)$  SWNT type were normalized to the intensity measured in hexane. The data shows considerable scatter but it is again clear that intensity decreases are dependent on the SWNT diameter. For example, the PL emission intensity of the (6,5), (9,5), and (10,5) SWNT types decrease by approximately 35%, 40%, and 65% in higher dielectric media, respectively. These results show that SWNT PL emission is very sensitive to polar solvents. For example, a large portion of the decrease in PL intensity for each  $(n,m)$  SWNT type is observed in chloroform, which has  $\epsilon \sim 5$ . The sensitivity of SWNT PL emission to polar environments could have significant implications in understanding the PL emission intensity from aqueous suspensions, where minor amounts of water in contact with the SWNT sidewall may significantly affect PL intensity. Indeed, researchers have found that better surfactant layers result in higher PL intensity.<sup>27–28,36</sup>

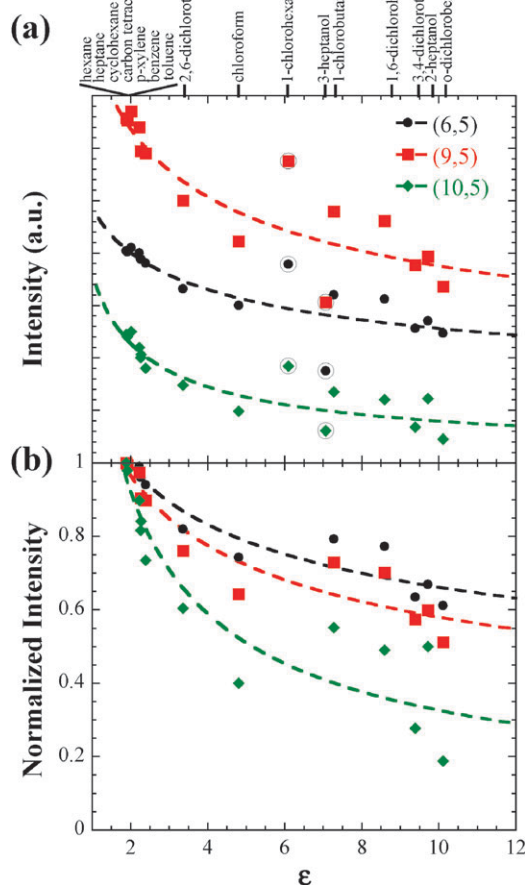


**Fig. 5** The PL emission (a) intensity and (b) normalized intensity for selected  $(n,m)$  SWNT types as a function of dielectric constant. The intensities in (a) are offset for clarity. The dashed lines are power law fits. The open circles in (a) indicate points excluded from the power law fit and the data in (b). The intensities in (b) were normalized to the intensity of the  $(n,m)$  type mixed with hexane.

The Stokes shift is defined as the difference between peak position in absorbance and PL emission spectra and is related to the solvent reorganization that occurs during photon absorption. All of the nonpolar microenvironments yielded small Stokes shifts of approximately 1–5 meV (see supplemental information†). These small Stokes shifts indicate that both the ground and excited states of the SWNTs are equally stabilized in the nonpolar solvents. The similarity in solvation could indicate that either the difference of the dipole moment between the ground and excited states is small or that solvent relaxation has not occurred prior to radiative recombination. This latter effect might be expected for a dipole oriented along the length of the nanotube, which would require the solvent to move long distances in order to align with the excited state dipole. No trends were observed for the Stokes shift but this could be attributed to the small values and the error associated with deconvoluting the spectra.

### Nonlinear optimization model for approximating the longitudinal polarizability

The  $E_{ii}$  transitions for each  $(n,m)$  SWNT type from either the PL or absorbance spectra can be used to estimate the SWNT polarizability or its functional form; however, the PL data is used because the  $(n,m)$  peaks are better resolved. Previously, Choi and Strano<sup>9</sup> concluded that the difference in SWNT polarizability used in eqn (1) is primarily determined by the longitudinal polarizability of the exciton (*i.e.*  $\Delta\alpha_{11} \approx \alpha_{11,\parallel}$ ). Several research groups have described the longitudinal polarizability of each SWNT  $(n,m)$  type by a function of the form,  $\alpha_{11,\parallel} = kR^a E_{11}^b$ , where  $k$  is a constant,  $a$  and  $b$  are

integers,  $R$  is the SWNT radius, and  $E_{11}$  is the band gap as measured in air.<sup>22–25</sup> As described above, there is no consensus on the relationship (*i.e.* constants  $a$  and  $b$ ) for the polarizability. If the volume associated with the excited state is assumed to be a sphere with a radius equivalent to the SWNT radius, then eqn (1) becomes:

$$\Delta E_{11} = \frac{-C_{\text{solvent}}}{\beta\gamma} kR^{a-3} E_{11}^b \Delta f = -D_{\text{solvent}} R^{a-3} E_{11}^b \Delta f \quad (2)$$

The constants  $C_{\text{solvent}}$ ,  $k$ ,  $\beta$ , and  $\gamma$  are combined into one constant  $D_{\text{solvent}}$  for simplicity. Since eqn (2) is valid for all solvents, the measured solvatochromic shifts in Fig. 1 can then be compared to this equation to determine the global variables,  $a$  and  $b$ , and the solvent specific variables,  $D_{\text{solvent}}$ .

All PL spectra in Fig. 1 were deconvoluted into their respective  $(n,m)$  peaks. The  $E_{11}$  transitions for each  $(n,m)$  SWNT type in air were subtracted from the  $E_{11}$  recorded from each spectrum in each solvent to give the solvatochromic shift ( $\Delta E_{11}$ ). The optical transitions in air were based on the equation developed by Choi and Strano.<sup>9</sup> As shown in Fig. S1,† there can be considerable overlap in the deconvoluted PL spectra for each  $(n,m)$  SWNT type. For example, the (7,6) SWNT type shown in Fig. S1a† has good intensity and little overlap with other  $(n,m)$  SWNT types. On the other hand, the (12,2) SWNT type in Fig. S1b† shows considerable overlap with other  $(n,m)$  types and low intensity. Therefore, the confidence level of each peak in the deconvoluted spectra was evaluated to assess its relative importance in regression analysis. To account for the varying confidence levels in each deconvoluted peak, weighting factors were assigned based on the relative intensity ( $w_{\text{Intensity}}$ ) and amount of overlap ( $w_{\text{Overlap}}$ ) in each solvent. This technique is often used in nonlinear optimization to account for the relative importance of data.<sup>37,38</sup> As shown in Table 2, both the intensity and overlap were broken up into three categories and assigned values of 1, 0.5, or 0.25. Fig. S1† shows some examples of those peaks associated with each category. These two weighting factors were multiplied together to get the weighting factors listed in Table 3 for all SWNT types in all solvents. The general trend shown in the table is that the (7,6) and (7,5)

**Table 2** Criterion for assigning the weighting factors for both intensity and amount of overlap with other peaks

Weighting factor	Area overlap	Intensity (662 nm excitation)	Intensity (784 nm excitation)
1	<50%	>0.4	>0.08
0.5	Between 50 and 100%	Between 0.2 and 0.4	Between 0.04 and 0.08
0.25	100%	<0.2	<0.04

**Table 3** Combined weighting factors ( $w = w_{\text{Intensity}} \cdot w_{\text{Overlap}}$ ) assigned for each  $(n,m)$  type as a function of solvent

Solvent	(6,5)	(8,3)	(7,5)	(7,6)	(10,2)	(9,4)	(11,1)	(8,6)	(9,5)	(12,1)	(11,3)	(12,2)	(10,5)	(9,7)
Hexane	0.5	0.5	1	1	0.5	0.25	0.25	0.25	0.5	0.25	1	0.25	1	1
Heptane	0.5	1	1	1	0.5	0.25	0.25	0.25	0.5	0.5	1	0.25	1	1
Cyclohexane	0.5	1	1	1	0.5	0.25	0.25	0.25	0.5	0.5	1	0.25	1	1
Carbon tetrachloride	0.5	0.5	1	1	0.5	0.25	0.25	0.25	0.5	0.25	1	0.25	1	1
p-Xylene	0.5	0.5	1	1	0.5	0.0625	0.25	0.25	0.5	0.125	1	0.25	1	0.5
Benzene	0.5	0.5	1	1	0.5	0.125	0.25	0.5	0.5	0.125	1	0.25	1	1
Toluene	0.5	0.5	1	1	0.5	0.125	0.25	0.5	0.5	0.125	1	0.25	1	0.5
2,6-Dichlorotoluene	0.5	0.5	0.5	1	0.5	0.125	0.0625	0.5	0.0625	0.0625	1	0.25	0.25	0.5
Chloroform	0.5	0.5	1	1	0.5	0.125	0.25	0.5	0.125	0.125	0.5	0.25	0.25	1
1-Chlorohexane	0.5	0.5	1	1	0.5	0.125	0.25	0.5	0.125	0.125	1	0.25	0.5	1
3-Heptanol	0.5	0.5	1	1	0.5	0.25	0.25	0.25	0.5	0.25	1	0.25	1	1
1-Chlorobutane	0.5	0.5	1	1	0.5	0.125	0.25	0.5	0.125	0.125	1	0.25	0.5	1
1,6-Dichlorohexane	0.5	0.5	1	1	0.5	0.125	0.25	0.5	0.125	0.0625	0.5	0.25	0.25	1
3,4-Dichlorotoluene	0.5	0.5	1	1	0.5	0.0625	0.25	0.5	0.25	0.0625	0.25	0.125	-	0.0625
2-Heptanol	0.5	0.5	1	1	0.5	0.25	0.25	0.25	0.5	0.25	1	0.25	1	1
o-Dichlorobenzene	0.5	0.5	1	1	0.5	0.125	0.25	0.5	0.125	0.0625	0.25	0.125	0.25	-
Average	<b>0.50</b>	<b>0.56</b>	<b>0.97</b>	<b>1.00</b>	<b>0.50</b>	<b>0.16</b>	<b>0.24</b>	<b>0.39</b>	<b>0.34</b>	<b>0.19</b>	<b>0.84</b>	<b>0.23</b>	<b>0.73</b>	<b>0.84</b>

spectra have the highest confidence while the (9,4) and (12,1) have the lowest in each solvent.

A constrained nonlinear optimization model was then formulated using the generalized reduced gradient (GRG) method.<sup>37</sup> An objective function ( $\phi$ ) was chosen to be the squared sum of residuals multiplied by the weighting factors ( $w_i$ ) where  $\Delta E_{11}$  are the measured shifts relative to air or the calculated values from eqn (1). These residuals were summed over all ( $n,m$ ) types and solvents to obtain the final objective function:

$$\min \phi = \sum_{\text{all solvents}} \sum_{\text{all } n,m} W_{\text{Intensity}}^{n,m} W_{\text{Overlap}}^{n,m} \times \left( \Delta E_{11,\text{measured}}^{n,m} - \Delta E_{11,\text{calculated}}^{n,m} \right)^2 \quad (3)$$

The objective function (3) was solved with all optimization variables constrained to values between  $-10$  and  $10$  to aid optimization. The global parameters  $a$  and  $b$  had the additional constraints of being integers. Central differences were used to calculate the partial derivatives of the objective function. The search direction was determined at each iteration by using the conjugate method. The objective function was considered to converge once the relative change between iterations was less than  $10^{-7}$ . A minimum of four different initial starting points for the parameters were used to obtain the global minimum rather than local minima.

In addition to the solution using data from all solvents, solutions using data from individual solvents were found independently to obtain the parameters  $a$ ,  $b$ , and  $D_{\text{solvent}}$ . Table 4 shows the results from all optimization calculations. Some optimization models had minima that were weak functions of the parameters  $a$  and  $b$ . In other words, the values of  $a$  and  $b$  could be changed by  $\pm 1$  without affecting the value of the objective function. For example, the optimization of only heptane gave solutions of  $a = -2$ ,  $b = -3$  and  $a = -3$ ,  $b = -4$ . However, one of these solutions coincided with the global optimization solution. Therefore, this data set was listed in Table 4. Nearly all optimization solutions yielded solutions of  $a = -2$  and  $b = -3$ . As seen in Table 4, a global solution with all weighting factors set equal to 1 gave a different solution. However, as described above, this solution is discarded because of the difference in data quality for each ( $n,m$ ) SWNT type. This analysis suggests that the longitudinal polarizability of the exciton should have the form,  $\alpha_{11,\parallel} = kR^{-2}E_{11}^{-3}$ . Inserting this relation into eqn (2) yields an expression for the solvatochromic shift:

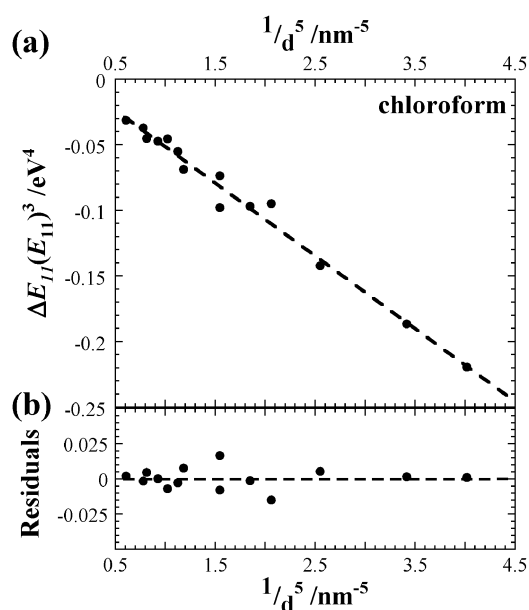
$$\Delta E_{11} = -D_{\text{solvent}} R^{-5} E_{11}^{-3} \Delta f \text{ or} \\ \Delta E_{11} E_{11}^3 = -D_{\text{solvent}} \Delta f / R^5 \quad (4)$$

Fig. 6a shows the fit to eqn (4) for the solvatochromic shift of SWNTs when surrounded by chloroform microenvironments. The linear fit yields  $R^2 = 0.98$ , indicating that the parameters for the polarizability expression show excellent agreement with the experimental data. As shown in Fig. 6b, the largest residuals are for the (11,1), (9,4), and (7,6) SWNT types; however, two of these nanotubes, the (11,1) and (9,4), have the same diameters, so a large error is associated with the deconvoluted peak positions, as indicated in Table 3.

**Table 4** Optimization results for all fitted parameters when solved as individual systems and collectively

Parameter <sup>a</sup>	All solvents	Hexane	Heptane <sup>b</sup>	Cyclohexane <sup>b</sup>	Carbon tetrachloride <sup>b</sup>	p-Xylene <sup>c</sup>	Benzene	Toluene	2,6-Dichloro-toluene	Chloroform	1-Chloro-hexane	3-Heptanol	1-Chloro-butane	1,6-Dichloro-hexane <sup>c</sup>	3,4-Dichloro-toluene	2-Heptanol	o-Dichloro-benzene	All solvents ( $w_i = 1$ ) <sup>d</sup>
$a$	-2	-2	-2	-2	-2	-2	-2	-2	0	-2	-2	-3	-2	-2	0	-3	-1	-3
$b$	-3	-3	-3	-3	-3	-3	-3	-3	-1	-3	-3	-4	-3	-3	-1	-4	-2	-4
$D_{\text{hexane}}$	4.1	4.1																2.2
$D_{\text{heptane}}$	3.9		3.9															2.1
$D_{\text{cyclohexane}}$	3.6			3.6														1.9
$D_{\text{carbon tetrachloride}}$	3.6				3.6													1.9
$D_{\text{p-xylene}}$	3.6					3.6												1.9
$D_{\text{benzene}}$	3.6						3.6											1.9
$D_{\text{toluene}}$	3.6							3.6										1.8
$D_{2,6\text{-dichlorotoluene}}$	3.6								13.3									2.0
$D_{\text{chloroform}}$	3.9									3.9								2.1
$D_{1\text{-chlorohexane}}$	4.0										4.0							2.0
$D_{3\text{-heptanol}}$	3.8											2.0						2.2
$D_{1\text{-chlorobutane}}$	4.1												4.1					2.0
$D_{1,6\text{-dichlorohexane}}$	3.9													3.9				1.9
$D_{3,4\text{-dichlorotoluene}}$	3.9														14.4			2.0
$D_{2\text{-heptanol}}$	3.8															2.0		2.0
$D_{o\text{-dichlorobenzene}}$	3.9															2.0	7.5	2.0

<sup>a</sup>  $D$  is given in  $\text{meV nm}^5 \text{eV}^3$ . <sup>b</sup> Minimum was weak function and also gave a possible solution of  $a = -3$  and  $b = -4$ . The listed solution was chosen since it was identical to the overall optimization parameter set for all solvents. <sup>c</sup> Minimum was weak function and also gave a possible solution of  $a = -1$  and  $b = -2$ . The listed solution was chosen since it was identical to the overall optimization parameter set for all solvents. <sup>d</sup> Optimization solution with all weighting factors set to 1. This solution is not recommended given the uncertainty in the deconvolution.



**Fig. 6** Solvatochromic shifts of SWNTs in chloroform microenvironments relative to air. (a) The polarizability parameters  $a$  and  $b$  determined from the nonlinear optimization yield a linear expression with (b) low residuals.

These results deviate from prior reports, which obtained values of  $a$  ranging from 2 to  $-1$  and  $b$  from 0 to  $-2$ .<sup>22–25</sup> However, note that those solutions that deviate from the other results tend to be the most polar solvents. The changes in intensity and peak position for these systems induce more error in peak assignment. On the other hand, some of these systems give  $a$  and  $b$  constants comparable to those obtained before.<sup>9,23</sup>

## Conclusion

Multiple solvents form microenvironments around SWNTs, inducing solvatochromic shifts that range from approximately 25 to 100 meV. The shifts scale well with the solvent induction polarization,  $f(\eta^2)$ , as expected for interactions of a polarizable SWNT with a polarizable solvent. The solvent microenvironments show the sensitivity of SWNT PL to slight changes in their environment. A change of the dielectric constant ( $\epsilon$ ) from 2 to 5 could result in a drop in PL intensity of more than 50%, which could have significant implications on the measured intensity of poorly coated SWNTs in aqueous environments. Changes to the environment have the most significant effect on the peak position of the smallest diameter SWNTs and the intensity of the largest diameter SWNTs. A constrained nonlinear optimization model was used to study the polarizability changes with each solvent microenvironment. The results yield a longitudinal polarizability of the form  $\alpha_{11,\parallel} \propto 1/(R^2 E_{11}^3)$ .

## Acknowledgements

We acknowledge the support of the Donors of the American Chemical Society Petroleum Research Fund and the National Science Foundation (CBET-0853347) for support of this

research. Carlos A. Silvera-Batista thanks SEAGEP at the University of Florida for their support. We gratefully thank Prof. Yiider Tseng for access to the ultracentrifuge, the Richard Smalley Institute at Rice University for supplying SWNTs, and Prof. Leon Lasdon for use of the GRG code.

## References

- 1 M. O'Connell, S. M. Bachilo, C. Huffman, V. C. Moore, M. S. Strano, E. Haroz, K. L. Rialon, P. Boul, W. H. Noon, C. Kittrell, J. Ma, R. H. Hauge, R. B. Weisman and R. Smalley, *Science*, 2002, **297**, 593.
- 2 R. Haggemueller, S. S. Rahatekar, J. A. Fagan, J. H. Chun, M. L. Becker, R. R. Naik, T. Krauss, L. Carlson, J. F. Kadla, P. C. Trulove, D. F. Fox, H. C. DeLong, Z. C. Fang, S. O. Kelley and J. W. Gilman, *Langmuir*, 2008, **24**, 5070.
- 3 V. C. Moore, M. S. Strano, E. H. Haroz, R. H. Hauge and R. E. Smalley, *Nano Lett.*, 2003, **3**, 1379.
- 4 S. M. Bachilo, M. S. Strano, C. Kittrell, R. H. Hauge, R. E. Smalley and R. B. Weisman, *Science*, 2002, **298**, 2361.
- 5 R. B. Weisman and S. M. Bachilo, *Nano Lett.*, 2003, **3**, 1235.
- 6 R. Bandyopadhyaya, E. Nativ-Roth, O. Regev and R. Yerushalmi-Rozen, *Nano Lett.*, 2002, **2**, 25.
- 7 P. T. Araujo and A. Jorio, *Phys. Status Solidi B*, 2008, **245**, 2201.
- 8 P. T. Araujo, I. O. Maciel, P. B. C. Pesce, M. A. Pimenta, S. K. Doorn, H. Qian, A. Hartschuh, M. Steiner, L. Grigorian, K. Hata and A. Jorio, *Phys. Rev. B: Condens. Matter Mater. Phys.*, 2008, **77**, 241403.
- 9 J. H. Choi and M. S. Strano, *Appl. Phys. Lett.*, 2007, **90**, 223114.
- 10 A. Jorio, I. O. Maciel, P. T. Araujo, P. B. C. Pesce and M. A. Pimenta, *Phys. Status Solidi B*, 2007, **244**, 4011.
- 11 O. Kiowski, S. Lebedkin, F. Hennrich, S. Malik, H. Rosner, K. Arnold, C. Surgers and M. M. Kappes, *Phys. Rev. B: Condens. Matter Mater. Phys.*, 2007, **75**, 075421.
- 12 M. J. Longhurst and N. Quirke, *J. Chem. Phys.*, 2006, **124**, 234708.
- 13 Y. Miyauchi, R. Saito, K. Sato, Y. Ohno, S. Iwasaki, T. Mizutani, J. Jiang and S. Maruyama, *Chem. Phys. Lett.*, 2007, **442**, 394.
- 14 Y. Ohno, S. Iwasaki, Y. Murakami, S. Kishimoto, S. Maruyama and T. Mizutani, *Phys. Status Solidi B*, 2007, **244**, 4002.
- 15 A. G. Walsh, A. N. Vamivakas, Y. Yin, S. B. Cronin, M. S. Unlu, B. B. Goldberg and A. K. Swan, *Nano Lett.*, 2007, **7**, 1485.
- 16 J. G. Duque, M. Pasquali, L. Cognet and B. Lounis, *ACS Nano*, 2009, **3**, 2153.
- 17 T. Hertel, A. Hagen, V. Talalaev, K. Arnold, F. Hennrich, M. Kappes, S. Rosenthal, J. McBride, H. Ulbricht and E. Flahaut, *Nano Lett.*, 2005, **5**, 511.
- 18 J. L. Bahr, E. T. Mickelson, M. J. Bronikowski, R. E. Smalley and J. M. Tour, *Chem. Commun.*, 2001, 193.
- 19 L. J. Li, R. J. Nicholas, R. S. Deacon and P. A. Shields, *Phys. Rev. Lett.*, 2004, **93**, 156104.
- 20 N. R. Tummala and A. Striolo, *ACS Nano*, 2009, **3**, 595.
- 21 E. J. Wallace and M. S. P. Sansom, *Nano Lett.*, 2007, **7**, 1923.
- 22 L. X. Benedict, S. G. Louie and M. L. Cohen, *Phys. Rev. B: Condens. Matter*, 1995, **52**, 8541.
- 23 E. N. Brothers, G. E. Scuseria and K. N. Kudin, *J. Phys. Chem. B*, 2006, **110**, 12860.
- 24 B. Kozinsky and N. Marzari, *Phys. Rev. Lett.*, 2006, **96**, 166801.
- 25 G. Y. Guo, K. C. Chu, D. S. Wang and C. G. Duan, *Comput. Mater. Sci.*, 2004, **30**, 269.
- 26 M. S. Brown, J. W. Shan, C. Lin and F. M. Zimmermann, *Appl. Phys. Lett.*, 2007, **90**, 203108.
- 27 R. K. Wang, W.-C. Chen, D. K. Campos and K. J. Ziegler, *J. Am. Chem. Soc.*, 2008, **130**, 16330.
- 28 J. L. Blackburn, T. J. McDonald, W. K. Metzger, C. Engtrakul, G. Rumbles and M. J. Heben, *Nano Lett.*, 2008, **8**, 1047.
- 29 L. Cognet, D. A. Tsybolski, J. D. R. Rocha, C. D. Doyle, J. M. Tour and R. B. Weisman, *Science*, 2007, **316**, 1465.
- 30 M. S. Strano, C. B. Huffman, V. C. Moore, M. J. O'Connell, E. H. Haroz, J. Hubbard, M. Miller, K. Rialon, C. Kittrell, S. Ramesh, R. H. Hauge and R. E. Smalley, *J. Phys. Chem. B*, 2003, **107**, 6979.

- 
- 31 T. H. Lowry and K. S. Richardson, *Mechanism and Theory in Organic Chemistry*, Benjamin-Cummings Publishing Company, New York, 1987.
- 32 P. Suppan, *J. Photochem. Photobiol., A*, 1990, **50**, 293.
- 33 P. Suppan and N. Ghoneim, *Solvatochromism*, The Royal Society of Chemistry, Cambridge, UK, 1997.
- 34 R. K. Wang, H.-O. Park, W.-C. Chen, C. Silvera-Batista, R. D. Reeves, J. E. Butler and K. J. Ziegler, *J. Am. Chem. Soc.*, 2008, **130**, 14721.
- 35 R. K. Wang, R. D. Reeves and K. J. Ziegler, *J. Am. Chem. Soc.*, 2007, **129**, 15124.
- 36 J. G. Duque, L. Cognet, A. N. G. Parra-Vasquez, N. Nicholas, H. K. Schmidt and M. Pasquali, *J. Am. Chem. Soc.*, 2008, **130**, 2626.
- 37 S. Smith and L. Lasdon, *ORSA J. Comput.*, 1992, **4**, 2.
- 38 K. J. Ziegler, J. Chlistunoff, L. Lasdon and K. P. Johnston, *Comput. Chem.*, 1999, **23**, 421.
- 39 D. R. Lide, *CRC Handbook of Chemistry and Physics*, CRC Press, Boca Raton, Florida, 80th edn, 1999.
- 40 K. E. Calderbank, R. J. W. Le Fèvre and R. K. Pierens, *J. Chem. Soc. B*, 1969, 968.
- 41 W. E. Vaughan, *Digest of Literature on Dielectrics*, National Academy of Sciences, Washington, DC, 1975.